3-15-2017

Liquid-Gas Surface Tension Voltage Dependence During Electrowetting on Dielectric of 5-90 nm Gold Nanofluids

Saeid Vafaei
Bradley University

Karthik Chinnathambi
Boise State University

Theodorian Borca-Tasciuc
Rensselaer Polytechnic Institute

Publication Information

Vafaei, Saeid; Chinnathambi, Karthik; and Borca-Tasciuc, Theodorian. (2017). "Liquid-Gas Surface Tension Voltage Dependence During Electrowetting on Dielectric of 5-90 nm Gold Nanofluids". *Journal of Colloid and Interface Science, 490*, 797-801.http://dx.doi.org/10.1016/j.jcis.2014.12.049

Liquid-gas surface tension voltage dependence during electrowetting on dielectric of 5-90 nm gold nanofluids

Saeid Vafaei[1*], Karthik Chinnathambi [2], Theodorian Borca-Tasciuc[3*]

[1]Department of Mechanical, Materials and Manufacturing, University of Nottingham, Nottingham, UK.

E-Mail: S.Vafaei@qmul.ac.uk

[2]Department of Materials Science and Engineering, Boise State University, Boise, USA.

[3]Department of Mechanical, Aerospace and Nuclear Engineering, Rensselaer Polytechnic Institute, Troy, NY, USA.

E-Mail: Borcat@rpi.edu
Tel: +1 518 276 2627

Abstract: This article investigates the effective liquid-gas surface tension changes of water and 5-90nm gold nanofluids measured during electrowetting on dielectric experiments. The Young-Laplace equation for sessile droplets in air was solved to fit the experimental droplet shape and determine the effective liquid-gas surface tension at each applied voltage. A good agreement between experimental droplet shapes and the predictions was observed for all the liquids investigated in applied range of 0-30V. The measured liquid-gas effective surface tensions of water and gold nanofluid decreased with voltage. At a given voltage, the effective liquid-gas surface tension of gold nanofluids initially decreased as the size of gold nanoparticles increased from 5 nm to 50 nm. Then, for 70nm and 90nm particle gold nanofluids, the effective liquid-gas surface tension started increasing too. The size of nanoparticles, and the applied voltage have a significant effect on variation of the effective liquid-gas surface tension with variations as much as 93% induced by voltage at a given particle size and 80% induced by particle size at a given voltage.

Keywords: Solid-liquid surface tension, Liquid-gas surface tension, Contact angle, Wettability, Electrowetting, Gold nanoparticle.

1. Introduction

The management of small amounts of liquids is essential for fluidic micro-electro-mechanical systems (MEMS) such as lab-on-chip and micro total analysis systems [1-4], microfluidic optics [5-6] and displays [7]. Several methods have been developed for microscale liquid management such as hydraulics [8], electrophoresis [9], electro-osmosis [10] and capillary driven phenomena [11] where liquid-gas and solid surface tensions are used to manage the liquid motion. The electrowetting phenomenon for liquid manipulation has raised a wide interest due to its applications in reading technology at micro scale, advanced lithography and complex photonics devices, microfluidic and nanofluidic liquid transportation, thermal management, wave guides, tunable micro lenses, controllable micromirrors, liquid displays, lab-on-chip and bio-MEMS [12-18].

In electrowetting experiments an electric field is applied between the liquid of interest and an underlying electrode. Redistribution of charges and dipoles at the liquid-solid interface change the effective liquid-solid surface tension and then the contact angle for a liquid droplet [19]. Electrowetting on dielectric (EWOD) has the potential to make larger changes in the contact angle, since an electrical insulator blocks the charge transfer between the liquid and the underlying electrode and electrolysis is eliminated. The droplet contact angle for a sessile droplet in air was observed to decrease [20] with increased voltage during electrowetting.

The challenges and applications of electrowetting have been explained in detail in references [20-22]. Several phenomena are reducing its level of reversibility [21], such as contact angle saturation [23], contact line instability and formation of small droplets at the contact line [24], flow inside micro-droplet [25-26] and non-equilibrium [26-27]. Several reasons have been proposed to explain the saturation phenomenon such as dielectric break down at higher voltage [28], the high charge density in the vicinity of the contact line [29], trapping charge effect [29], air ionization near the contact line [30], the effect of liquid resistivity [31] and fluid flow inside the droplet [25]. In addition, the roughness of the surface may affect the instability of the triple line [24] and contact angle hysteresis [32]. The effect of surface roughness on contact angle has been considered by Wenzel and Cassie-Baxter equations [33-36]. The conditions [37], uncertainties [38-39] and the use of correct form of these equations have been discussed in detail in reference [40].

Figure 1 shows schematically the force balance at the triple line of a sessile

droplet. The balance of liquid-gas and solid surface tensions forces typically defines the contact angle when gravity and surface roughness does not play a critical role.

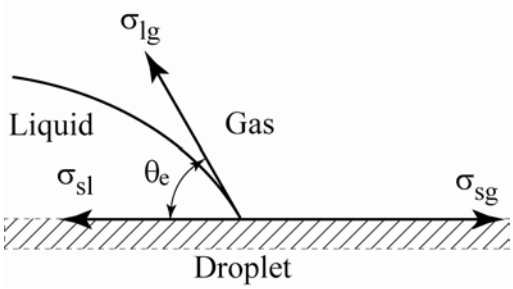

Figure 1. Schematic of effective forces at the triple line due to the liquid-gas and solid surface tensions.

When gravity becomes important [41], it favors the spreading of liquids on solid substrates and the reduction of contact angle. Practically, the droplet contact angle was observed decrease with increasing volume [42-43].

Suspended nanoparticles in the liquid host were observed to change the effective liquid-gas [44] and solid surface tensions [45] as well as the sessile droplet contact angle [46]. Similar results were observed in bubble growth experiments inside gold, silver and alumina nanofluids [41, 47-52]. The distribution of nanoparticles at the triple region is believed to play a major role in these experiments. Nanofluids have been found to have a different spreading and thinning (layering) behavior in the triple region compared to the pure liquids. The number of layers of nanoparticles (thickness) decreases in a stepwise pattern towards the triple line edge. The distribution of nanoparticles depends on the characteristics of nanoparticles, nanoparticle concentration, nanoparticle charge, solid-liquid-gas materials and film depth at the triple region [53-54]. It has been shown theoretically that particles can spread the triple line to a distance 20-50 times of the particle diameter through a structural disjoining pressure by self-ordering of particles in a confined wedge. However, the structural disjoining force only becomes significant at relatively high particle concentrations, i.e. over 20 vol. % [55].

Given the effects of nanoparticles on wetting and the strong interdependence between electrowetting and triple line phenomena, it is expected that nanoparticles play a major role in electrowetting. Most electrowetting experiments with nanofluids performed so far have focused on the contact angle [25, 20-21] of bismuth telluride

and silver nanofluids [20]. Major questions remain of what components of surface tension contribute to the contact angle changes. While typically it was assumed that the effective liquid-solid surface tension is responsible for the contact angle changes in electrowetting [19], this paper demonstrates strong effects of the applied voltage on the effective liquid-gas surface tension in water with and without suspended gold nanoparticles of 5-90nm diameters. This finding shines new light on the understanding of electrowetting experiments.

2. Experimental data

Figure 2 shows a schematic of the experimental setup. A Si (100) substrate was coated with 100 nm of Si_3N_4 and 1.2 μm hydrophobic layer of AF Teflon solution (1% solute solution from Dupont). The mean roughness of the substrate was measured to be 0.51 nm, using tapping mode atomic force microscopy (AFM) [20]. The pure water and gold nanofluid droplets were injected on top of the coated substrate slowly and then a DC voltage was applied and gradually increased.

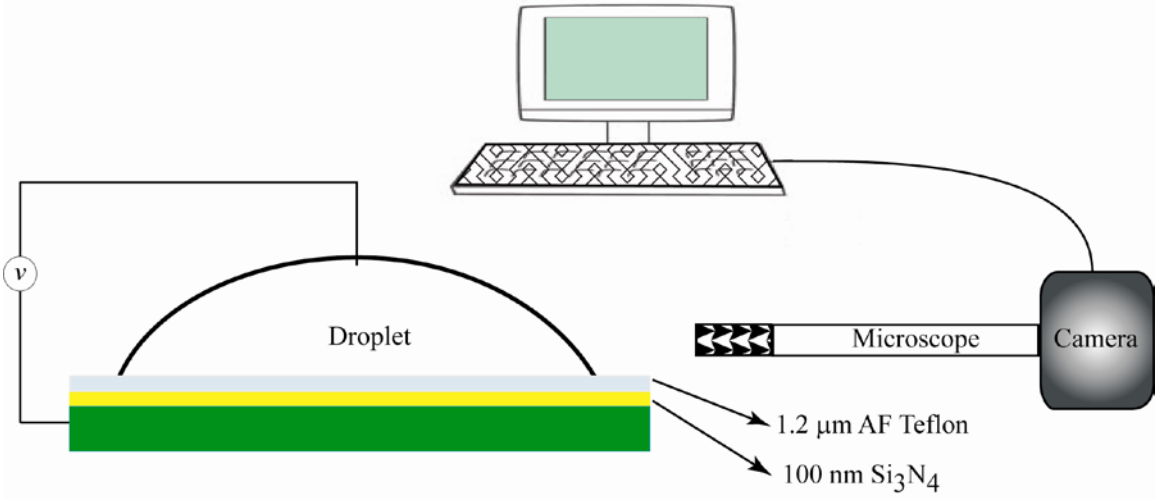

Figure 2. Schematic of experimental setup.

Gold nanoparticles of 5 nm, 30nm, 50 nm, 70 nm and 90 nm diameter were dispersed in DI water. The nanoparticles were functionalized by the manufacturer with a proprietary carboxylic acid and the solution could contain less than 0.1% of residual hydroxides. The concentration for all the gold nanofluids tested was $44\ \mu g / ml$.

A Nikon D100 camera equipped with a 7× optical zoom lens was employed to capture side-view high resolution images of the droplets during the electrical actuation. The pictures were captured a few seconds after applying the DC voltage to

ensure the steady state contact angle was reached. The droplet shape was captured during an applied voltage between 0-30 volts.

3 Prediction of the droplet shape

The Young-Laplace equation has been employed to predict the droplet shape both with [45-46] and without [42, 56] the presence of suspended nanoparticles. The Young-Laplace equation for droplets is,

$$\frac{d\theta}{ds} = \frac{2}{R_o} + \frac{gz}{\sigma_{\lg}}(\rho_l - \rho_g) - \frac{\sin\theta}{r} \tag{1}$$

The details of derivation of the Young-Laplace equation for droplets can be seen in references [46-47]. The Young-Laplace equation has been also applied successfully to predict bubble shapes [50-52]. In the case of nanofluids, the liquid-gas surface tension, $\sigma_{\lg}$ in Eq. 1 was replaced by the effective liquid-gas surface tension of nanofluids, $\sigma_{\lg n}$. To obtain the droplet shape, the Young-Laplace equation was solved with the following system of ordinary differential equations for axisymmetric interfaces.

$$\frac{dr}{ds} = \cos\theta \tag{2}$$

$$\frac{dz}{ds} = \sin\theta \tag{3}$$

$$\frac{dV}{ds} = \pi r^2 \sin\theta \tag{4}$$

This system of ordinary differential equations avoids the singularity problem at the bubble apex, since,

$$\left.\frac{\sin\theta}{r}\right|_{s=0} = \frac{1}{R_o} \tag{5}$$

where R_o is radius of curvature at apex.

The Young-Laplace equation can be applied to predict the droplet shape while the solid surface is smooth and homogenous. The Young-Laplace equation was also used to calculate the liquid-gas surface tension of nanofluids, knowing maximum radius of droplet, r_m, height of lateral apex, δ_m, and using the boundary conditions

$$r(0) = z(0) = \theta(0) = V(0) = 0 \tag{6}$$

The system of ordinary differential equations (1-4) was solved to obtain the axisymmetric droplet shape, using radius of triple line, droplet height and boundary

conditions (6). A similar method has been employed to calculate the liquid-gas surface tension in reference [44] and droplet shapes in references [42, 46, 56]. The Young-Laplace equation has been also employed in the presence of an electric field [57].

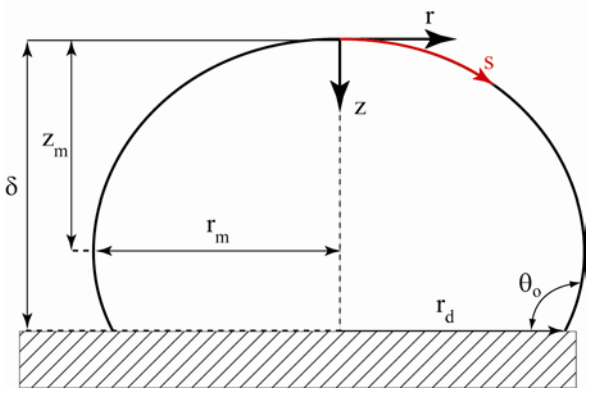

Figure 3. Schematic of a droplet shape.

4. Results and discussion

The characteristics of droplet shape such as radius of triple line, r_d , droplet height δ , and the location of lateral apex, (r_m, z_m) (seen in Figure 3) were measured, using captured images of droplets for the entire voltage range. Knowing characteristics of the droplet, the system of ordinary differential equations (1-4) was solved to predict the droplet shape and extract the effective liquid-gas surface tension as a function of voltage. Figure 4 shows good agreement between experimental droplet shapes and the predictions of droplet shapes, after solving the system of ordinary differential equations (1-4).

Figures 5 and 6 present the measured dependence of the effective liquid-gas surface tensions of water and gold nanofluids with applied voltage. Similarly, Fig. 7 depicts the variation of the effective liquid-gas surface tension of gold nanofluids with nanoparticle size. The experimental uncertainty for the fitted surface tension was estimated to be less than 6.5%. Under an applied electric field, the effective liquid-gas surface tension of water was found to decrease with voltage with a variation of as much as 83% over the entire range. The surface tension measured at 0 volts is within 0.1% of the reference value. The largest change in the effective surface tension occurs between 0 and 10V after which the changes are more gradual. The reduction of liquid-gas surface energy might be attributed to the presence of repulsion forces between counter-ions that start to accumulate near liquid-gas interface adjacent to the top

electrode as soon as a voltage is applied. The higher applied voltage, the higher is the charge density at the liquid-gas interface and therefore the larger the decrease in surface energy. The change in surface charge density seems to occur more strongly for the first voltage increment. Similar to the result presented here the effective liquid-gas surface tension of pure water was observed to decrease in electric fields due to excess electric charges [58]. The electric field has been also predicted to change the molecular O-H bound lengths and the angle of H-O-H bound [59], however the applied fields were much larger than in our experiments.

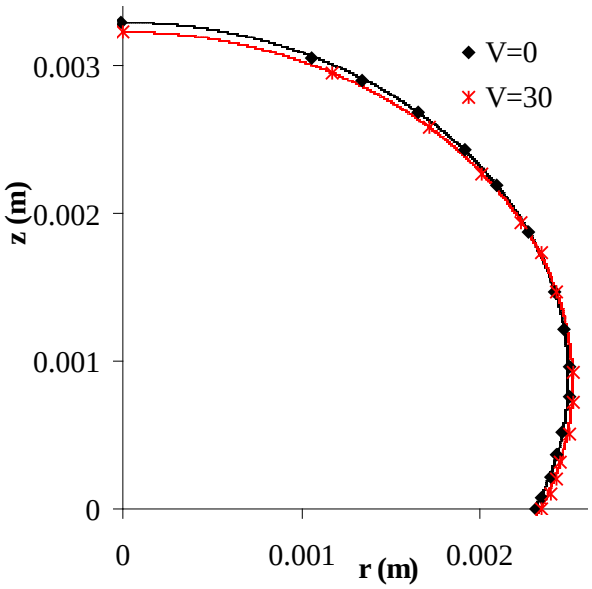

Figure 4. Comparison of experimental data with prediction of droplet shape using the fitted values of the effective surface tension and when voltage is zero and 30 volts, respectively. The size of nanoparticles is 90 nm.

Figure 6 shows the effects of the size of nanoparticles and voltage on the effective liquid-gas surface tension of gold nanofluids. At a given voltage, the effective liquid-gas surface tension of gold nanofluids initially decreased as the size of gold nanoparticles increased from 5 nm to 50 nm. Then for 70nm and 90nm particle, the effective liquid-gas surface tension started increasing too. Effective surface tension changes are as much as 93% induced by voltage at a given particle size and 80% induced by particle size at a given voltage

There are multiple avenues to affect the surface energy in complex liquids such as the gold nanofluids tested in this work. These changes may be connected to the presence and interactions between nanoparticles distributed on the droplet surface, in addition to ionic charges and perhaps residual surfactants from the host liquid that

distribute at the liquid-gas interface. The organization of nanoparticles on the liquid-gas interface depends on the equilibrium between repulsive and attractive forces among nanoparticles, as well as forces driving the diffusion of nanoparticles near the interface. The electrostatic forces serve as repulsive forces and Van der Waals forces may serve as attractive forces. Nanoparticle agglomeration and assembly near liquid-gas interfaces, was proposed to be responsible for the observed changes in the effective liquid-gas surface tension of nanofluids under no electric field [44]. It is possible that the assembly of nanoparticles may change under an applied electric field giving rise to the experimentally observed trends. For all nanofluids the liquid-gas surface tension decreased with the applied voltage, which is similar to the trend observed for water, including the sharpest decrease at the first voltage increment and is perhaps mainly due to the distribution of the ionic charges intrinsic to the host solution, although redistribution of nanoparticles on the surface with voltage could be an alternative explanation. The nanoparticle redistribution effect could be also superposed onto a surface ionic charge distribution effect. It is observed that at zero voltage the effective gas-liquid surface tension of all nanofluids was higher than water and decreased monotonically as the particle size increased (see Figure 7). These results could indicate the presence of nanoparticles at the liquid-gas interface. At locations where nanoparticles are breaking through the interface, the gas-liquid contribution to surface energy is replaced by solid-gas contributions from nanoparticles. For wetting cases, the typical values of gas-solid surface tensions [41-42, 45-46] are larger than the gas-water surface tensions, potentially explaining the observed increase in the effective surface tension with addition of gold nanoparticles. As soon as the first voltage increment was applied, the trend of nanoparticle size vs. effective surface tension was broken by the 70 nm and 90 nm nanoparticles. The 90 nm gold nanofluid experienced a much less decrease in surface tension compared to the rest of the nanofluids as shown in Figure 6. This trend is perhaps explained by the effect of the applied voltage on the distribution of nanoparticles at the gas-liquid interface as well as the surface energy. Different size nanoparticles are likely to organize differently and perhaps the larger size nanoparticles are somewhat less susceptible to large changes under electrostatic interactions than their smaller counterparts. While the discussion above provides several possible mechanisms to explain the observed experimental trends, more studies, including nanoparticle distribution under electric field are required to understand the surface tension

dependence with electric field in nanofluids.

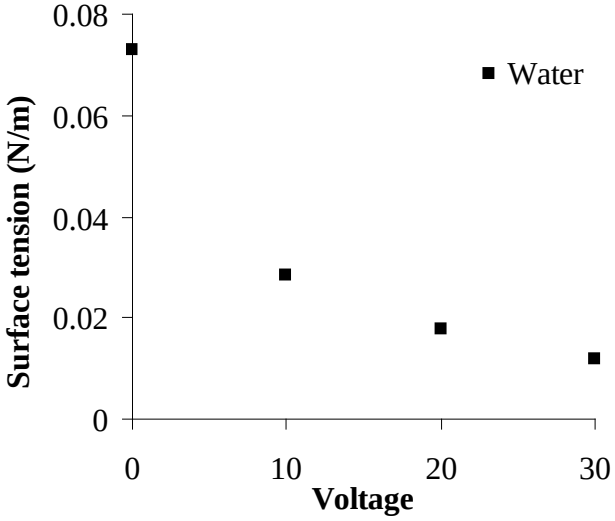

Figure 5. Variation of the effective liquid-gas surface tension with applied voltage for water.

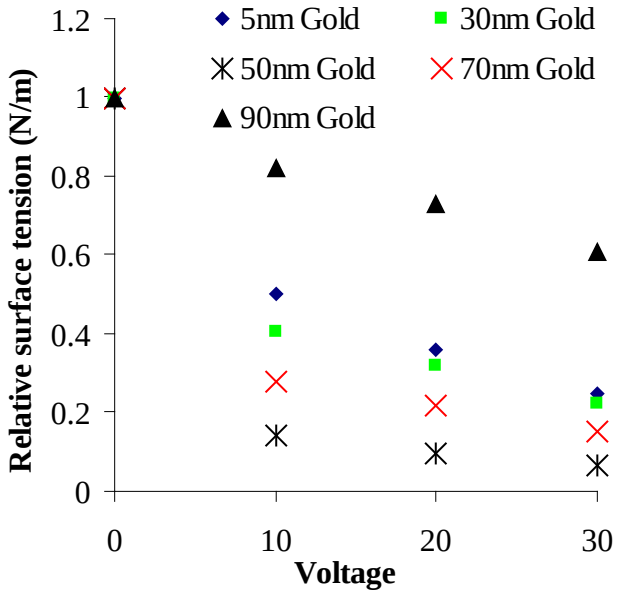

Figure 6. Variation of the effective liquid-gas surface tension with applied voltage and size of the gold nanoparticles.

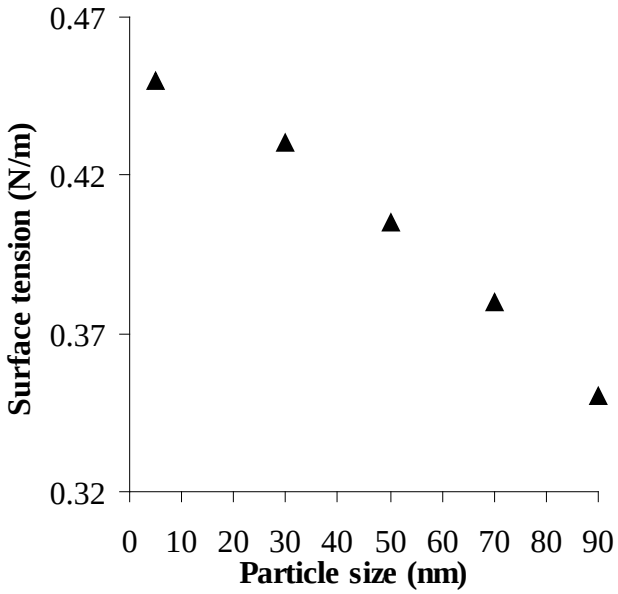

Figure 7. Variation of the effective liquid-gas surface tension with size of gold nanoparticles at zero voltage.

5. Conclusions

Water and gold nanofluids were employed to study the effects of applied voltage and the size of gold nanoparticles on the effective liquid-gas surface tension during electrowetting on dielectric experiments. The Young-Laplace equation was able to successfully predict the droplet shape and was used to extract the effective liquid-gas surface tension in the range of 0-30 V. The effective liquid-gas surface tension of water and gold nanofluid was found to decrease with the applied voltage. For a given voltage, the effective liquid-gas surface tension of gold nanofluids decreased as size of nanoparticles increased from 5 nm to 50 nm and it started increasing, as size of nanoparticles increased further (from 50 nm to 90 nm). At zero voltage, the effective surface tension of all gold nanofluids decreased monotonically as the particle size increased.

Nomenclature

d Dielectric thickness $[m]$

g Acceleration of gravity $[m/s^2]$

R_o Radius of curvature at origin $[m]$

r_d Radius of contact line of droplet $[m]$

V Volume of droplet $[m^3]$

v Voltage $[v]$

Greek Symbols

δ Droplet hight $[m]$

ε Dielectric constant

θ_o Equlibruim contact angle

ρ_l Liquid density $[kg/m^3]$

σ_{sg} Solid-gas surface tension $[N/m]$

σ_{sl} Solid-liquidsurface tension $[N/m]$

σ_{lg} Gas-liquid surface tension $[N/m]$

References

[1] K. C. Sung, M. Hyejin, K. Chang-Jin, Creating, transporting, cutting, and merging liquid droplets by electrowetting-based actuation for digital microfluidic circuits, J. Microelectromech. Syst. 12 (2003) 70-80.

[2] Z. Yuejun, K. C. Sung, Microparticle sampling by electrowetting- actuated droplet sweeping, Lab Chip 6 (2006) 137-144.

[3] C. G. Cooney, C. Chao-Yi, M. R. Emerling, A. Nadim, J. D. Sterling, Electrowetting droplet microfluidics on a single planar surface, Microfluid Nanofluid, 2 (2006) 435-446.

[4] M. G. Pollack, R. B. Fair, A. D. Shenderov, Electrowettingbased actuation of liquid droplets for microfluidic applications, Appl. Phys. Lett. 77 (2000) 1725-1726.

[5] S. Kuiper, B. H. Hendriks, Variable-focus liquid lens for miniature cameras, Appl. Phys. Lett. 85 (2004) 1128-1131.

[6] T. Krupenkin, S. Yang, P. Mach, Tunable liquid microlens, Appl. Phys. Lett. 82 (2003) 316-319.

[7] A. H. Robert, B. J. Feenstra, Video-speed electronic paper based on electrowetting, Nature 425 (2003) 383-385.

[8] S. Mutzenich, T. Vinay, G. Rosengarten, Analysis of a novel micro-hydraulic actuation for MEMS, Sensors Actuators A. 116 (2004) 525-529.

[9] S. Ghosal, Fluid mechanics of electroosmotic flow and its effect on band broadening in capillary electrophoresis, Electrophoresis 25 (2004) 214-228.

[10] W. E. Morf, O. T. Guenat, N. F. B. de Rooij, Sensors Actuators 72 (2001) 266

[11] T. M. Squires, S. R. Quake, Microfluidics: Fluid physics at the nanoliter scale, Rev. Mod. Phys. 77 (2005) 977-1026

[12] C. Quilliet, B. Berge, Electrowetting: a recent outbreak, Curr. Opin. Colloid Interface Sci. 6 (2001) 34-39.

[13] B. Berge, J. Peseux, Variable focal lens controlled by an external voltage: an application of electrowetting, Eur. Phys. J. E3 (2000) 159-163.

[14] J. Lee, C. J. Kim, Surface-tension-driven microactuation based on continous electrowetting, J. Microelectromech. Syst. 9 (2000) 171-180.

[15] J. Lee, H. Moon, J. Fowler, T. Schoellhammer, C. J. Kim, Electrowetting and electrowetting-on-dieletric for microscale liquid handling, Sens. Actuators A, 95 (2002) 259-268.

[16] J. F. Shackleford, W. Aexander, CRC Materials Science and Engineering Handbook 3rd ed. Boca Raton, FL: CRC Press 2000.

[17] P. Krulevitch, A. P. Lee, P. B. Ramsey, J. C. Trevino, J. Hamilton, M. A. Northrup, Thin film shape memory alloy microactuators, J. Microelectromech. Syst. 5 (1996) 270-282.

[18] R. H. Wolf, A. H. Tini Heuer, (shape memory) films on silicon for MEMS applications, J. Microelectromech. Syst. 4 (1995) 206-212.

[19] A. Adamson, Physical Chemistry of Surfaces, Third Edition, John Wiley & Sons, New York, 1976.

[20] R. K. Dash, T. Borca-Tasciuc, A. Purkayastha, G. Ramanath, Electrowetting on dielectric-actuation of microdroplets of aqueous bismuth telluride nanoparticle suspensions, Nanotechnology, 18 (2007) 475711-6.

[21] R. K. Dash, Microfluidic lens actuation via enhanced electrowetting on dielectric (EWOD), PhD Thesis, Rensselaer Polytechnic Institute, 2006.

[22] F. Mugele, J. C. Baret, Electrowetting: from basics to applications, Journal of Physics: Condensed Matter 17 (2005), 705-774.

[23] H. Moon, S. K. Cho, R. L. Garrell, C. J. Kim, Low voltage electrowetting-on-dielectric, J. Appl. Phys. 92 (2002) 4080-4087.

[24] F. Mugele, S. Herminghaus, Electrostatic stabilization of fluid microstructures, Appl. Phys. Lett. 81 (2002) 2303–2305.

[25] J. Lin, G. Lee, Y. Chang, K. Lien, Model description of contact angles in electrowetting on dielectriclayers, Langmuir 22 (2006) 484-489.

[26] O. Raccurt, J. Berthier, P. Clementz, M. Birella, M. J. Plissonnier, Micromech. Microeng. 17 (2007) 2217-2223.

[27] A. Patist, S. G. Oh, R. Lueng, D. O. Shah, Kinetics of miscellization: its significance to technological processes, Colloid Surf. A-Physicochem. Eng. Asp. 176 (2001) 3-16.

[28] A. G. Papathanasiou, A. G. Boudouvis, Manifestation of the connection between dielectric breakdown strength and contact angle saturation in electrowetting, Appl. Phys. Lett. 86 (2005) 1641021-3.

[29] H. J. J. Verheijen, M. W. J. Prins, Reversible electrowetting and trapping of charge: model and experiments, Langmuir 15 (1999) 6616-6620.

[30] M. Vallet, M. Vallade, B. Berge, Limiting phenomena for the spreading of water on polymer films by electrowetting, Eur. Phys. J. B. 11 (1999) 583-591.

[31] H. M. Shapiro, R. L. Garell, C. J. Kim, Equilibrium behavior of sessile drops under surface tension, applied external fields, and material variations, J. Appl. Phys. 93 (2003) 5794-5811.

[32] J. Chen, S. M. Troian, A. A. Darhuber, S. Wanger, Effect of contact angle hysteresis on thermocapillary droplet actuation, J. Appl. Phys. 97 (2005) 014906-1/9.

[33] A. B. D. Cassie, Discussions of the Faraday Society, 3 (1948) 11-16.

[34] S. Baxer, A. B. D. Cassie, Journal of Text. Inst. 36T (1945) 67-90.

[35] A. B. D. Cassie, S. Baxter, Trans. Faraday Soc. 40 (1944) 546-551.

[36] R. N. Wenzel, Resistance of solid surfaces to wetting by water, Indus. Eng. Chem. 28 (1936) 988-994.

[37] A. Marmur, E. Bittoun, When Wenzel and Cassie are right: Reconciling local and global considerations, Langmuir 25 (2009) 1277-1281.

[38] L. Gao, T. J. McCarthy, How Wenzel and Cassie were wrong, Langmuir 23 (2007) 3762-3765.

[39] L. Gao, T. J. McCarthy, An attempt to correct the faulty intuition perpetuated by the Wenzel and Cassie “laws”, Langmuir 25 (2009) 7249-7255.

[40]A. J. B. Milne, A. Amirfazli, The Cassie equation: How it is meant to be used, Adv. Colloid Interface Sci. 170 (2012) 48-55.

[41] S. Vafaei, D. Wen, Spreading of triple line and dynamics of bubble growth inside nanoparticle dispersions on top of a substrate plate, J. Colloid Interface Sci. 362 (2011) 285-291.

[42] A. W. Neumann, J. K. Spelt, Applied Surface Thermodynamics, M. Dekker, 1996.

[43] J. Gaydos, J; A. W. Neumann, The dependence of contact angles on drop size and line tension, J. Colloid Interface Sci. 120 (1987) 76-86.

[44] S. Vafaei, A. Purkayastha, A; Jain, G. Ramanath, T. Borca-Tasciuc, The effect of nanoparticles on the liquid-gas surface tension of Bi_2Te_3 nanofluids, Nanotechnology 20 (2009) 185702-185708.

[45] S. Vafaei, D. Wen, T. Borca-Tasciuc, Nanofluids surface wettability through asymptotic contact angle, Langmuir 27 (2011) 2211-2218.

[46] S. Vafaei, T. Borca-Tasciuc, M. Z. Podowski, A. Purkayastha, G. Ramanath, P. M. Ajayan, Effect of nanoparticles on sessile droplet contact angle, Nanotechnology 17 (2006) 2523-2527.

[47] S. Vafaei, D. Wen, Effect of gold nanoparticles on the dynamics of gas bubbles, Langmuir 26 (2010) 6902-6907.

[48] S. Vafaei, D. Wen, The effect of gold nanoparticles on the spreading of triple line, Microfluid. Nanofluid. 8 (2010) 843-848

[49] S. Vafaei, D. Wen, Bubble formation in a quiescent pool of gold nanoparticle suspension, Adv. Colloid Interface Sci. 159 (2010) 72-93.

[50] S. Vafaei, P. Angeli, D. Wen, Bubble growth rate from stainless steel substrate and needle nozzles, Colloid Surf. A-Physicochem. Eng. Asp. 387 (2011) 240-247.

[51] S. Vafaei, T. Borca-Tasciuc, D. Wen, Theoretical and experimental investigation of quasi-steady-state bubble growth on top of submerged stainless steel nozzles, Colloid Surf. A-Physicochem. Eng. Asp. 369 (2010) 11-19.

[52] S. Vafaei, D. Wen, Bubble formation on a submerged micronozzle, J. Colloid Interface Sci. 343 (2010) 291-297.

[53] D. T. Wasan, A. D. Nikolov, Spreading of nanofluids on solids, Nature 423 (2003) 156-159.

[54] A. Nikolov, K. Kondiparty, D. T. Wasan, Nanoparticle self-structuring in a nanofluid film spreading on a solid surface, Langmuir 26 (2010) 7665-7670.

[55] A. Chengara, D. Nikolov, D. T. Wasan, A. Trokhymchuk, D. Henderson, Spreading of nanofluids driven by the structural disjoining pressure gradient, J. Colloid Interface Sci. 280 (2004) 192-201.

[56] S. Vafaei, M. Z. Podowski, Analysis of the relationship between liquid droplet size and contact angle, Adv. Colloid Interface Sci. 113 (2005) 133-146.

[57] A. Bateni, S. S. Susnar, A. Amirfazli, A. W. Neumann, Development of a new methodology to study drop shape and surface tension in electric fields, Langmuir 20 (2004) 7589-7597.

[58] L. P. Santos, T. R. D. Ducati, L. B. S. Balestrin, F. Galembeck, Water with excess electric charge, J. Phys. Chem. C. 115 (2011) 11226-11232.

[59] S. Shun-Ping, Z. Quan, Z. Li, W. Rong, Z. Zheng-He, J. Gang, F. Yi-Bei, Geometrical structures, vibrational frequencies, force constants and dissociation energies of isotopic water molecules (H2O, HDO, D2O, HTO, DTO, and T2O) under dipole electric field, Chinese Physics B. 20 (2011) 063102-7.